Journal of Computational Physics **173,** 1–16 (2001)
doi:10.1006/jcph.2001.6834, available online at http://www.idealibrary.com on IDEAL®

A Second-Order Accurate, Component-Wise TVD Scheme for Nonlinear, Hyperbolic Conservation Laws

Heng Yu* and Yu-Ping Liu†

**Institute of Applied Physics and Computational Mathematics, Beijing, P. R. China; and Department of Mechanics and Engineering Science, Fudan University, Shanghai, P. R. China; and †Department of Applied Physics, Beijing University of Aeronautics and Astronautics, Beijing, P. R. China*
E-mail: yu_heng@china.com

Received April 17, 2000; revised May 18, 2001

In this paper, we present a two-step, component-wise TVD scheme for nonlinear, hyperbolic conservation laws, which is obtained by combining the schemes of Mac Cormack and Warming-Beam. The scheme does not necessitate the characteristic decompositions of the usual TVD schemes. It employs component-wise limiting; hence the programming is much simpler, especially for complicated coupled systems. For Euler systems of conservation laws, we found the scheme is two times faster in computation than the usual TVD schemes based on field-by-field decomposition limiting. A lot of numerical results show primarily the value of the new method.

Key Words: TVD; component-wise; conservation laws.

1. INTRODUCTION

Harten's concept of total variation diminishing (TVD) [1] initiated a new era of high-order and high-resolution schemes for hyperbolic conservation laws. TVD schemes are a kind of monotonicity preserving schemes by adding and limiting a modified, high-order antidiffusion term to a low-order (e.g., first-order upwind) numerical flux. They produce a high-resolution of discontinuities while retaining high-order accuracy in smooth regions.

Generally for the scalar case, the TVD technique is elegant and amenable to rigorous analysis. However, when applied to systems of conservation laws, TVD schemes are often built upon field-by-field decompositions. One extends the scalar scheme to systems of conservation laws by applying it "scalarly" to each of the (appropriately linearized) characteristic variables. However, this complicates the programming, increases the CPU time, and does not perform as well as the scalar case.

0021-9991/01 $35.00

Early shock capturing schemes for hyperbolic conservation laws (e.g., artificial viscosity methods) were mainly component-wise. The advantages of component-wise schemes are apparent: easier programming, faster computation, and wider applicability for complicated systems. Profited from a TVD Runge–Kutta type of time discretizations, the ENO schemes [11–14] had tried component-wise differencing which is obviously more efficient than characteristic-based TVD schemes.

We note that, for the custom, second-order, finite difference schemes of hyperbolic equations, oscillations of a central scheme and a bias (upwind) scheme always take place at opposite sides of a discontinuity. So spurious oscillations should vanish via some selective employments of the second-order schemes. Actually a TVD scheme often contains a switch that changes the scheme from one to another when some critical conditions are present. It is also known that a multi-step high-order scheme shares the merits of not using the Jacobian matrix. Naturally we propose a two-step, component-wise TVD scheme based on the well-known schemes of Mac Cormack and Warming-Beam.

The purpose of this paper is to show the simplicity and practicability of the new scheme. In the next section we describe this second-order (perhaps first-order at extrema), two-step component-wise, point-value version, TVD scheme. Then we exhibit some numerical results for nonlinear hyperbolic conservation laws.

2. TWO-STEP, COMPONENT-WISE TVD SCHEMES

2.1. *Review of the Usual TVD Limiting*

As preliminaries we shall first review the limiting procedure of the usual TVD schemes. Two versions of TVD techniques may be observed: TVD upwinding [2–7] and the symmetric TVD schemes [19]. Here we consider the former. For the linear scalar equation

$$u_t + au_x = 0, \quad a > 0. \tag{2.1}$$

The second-order Lax–Wendroff scheme may be written as

$$u_j^{n+1} = u_j^n - \nu\left(u_j^n - u_{j-1}^n\right) - \frac{1}{2}\nu(1-\nu)\left(u_{j+1}^n - 2u_j^n + u_{j-1}^n\right), \tag{2.2}$$

where $\nu = a\Delta t/\Delta x$ is the *CFL* number.

The scheme can be regarded as a first-order upwind scheme with an additional second-order antidiffusive term. Since the Lax–Wendroff scheme is not TVD, Sweby [2] modified it by adding a limiter to the second-order term

$$u_j^{n+1} = u_j^n - \left(u_j^n - u_{j-1}^n\right)\left[\nu + \frac{1}{2}\nu(1-\nu)\left(\frac{\varphi\left(r_{j+1/2}\right)}{r_{j+1/2}} - \varphi\left(r_{j-1/2}\right)\right)\right], \tag{2.3}$$

where the slope ratio is defined by

$$r_{j+1/2} = \frac{u_j^n - u_{j-1}^n}{u_{j+1}^n - u_j^n}. \tag{2.4}$$

Thereby the sufficient condition (see [1]) of (2.3) to be TVD becomes

$$-\frac{2}{1-\nu} \le \frac{\varphi\left(r_{j+1/2}\right)}{r_{j+1/2}} - \varphi\left(r_{j-1/2}\right) \le \frac{2}{\nu}. \tag{2.5}$$

More rigidly, if the *CFL* number ν is not fixed (under *CFL* condition $0 \le \nu \le 1$), then the TVD condition reduces to

$$\left| \frac{\varphi(r_{j+1/2})}{r_{j+1/2}} - \varphi(r_{j-1/2}) \right| \le 2. \tag{2.6}$$

When a limiter $\varphi(r)$ satisfying (2.5) is applied to (2.3), a second-order oscillation-free TVD scheme can be easily obtained.

For nonlinear scalar case

$$u_t + f(u)_x = 0, \tag{2.7}$$

we shall always approximate it by the following high-order conservative scheme

$$u_j^{n+1} = u_j^n - \lambda(\hat{h}_{j+1/2} - \hat{h}_{j-1/2}). \tag{2.8}$$

Here $\lambda = \Delta t/\Delta x$ is the uniform mesh ratio; $\hat{h}_{j+1/2}$ is a consistent, high-order numerical flux which can be also regarded as the numerical flux of a first-order upwind scheme with an additional higher order modified term; i.e.,

$$\hat{h}_{j+1/2} = \hat{f}_{j+1/2} + \frac{1}{2}\hat{g}_{j+1/2}. \tag{2.9}$$

Sweby [2] introduced flux TVD limiters for both positive and negative fluxes. The modified Lax–Wendroff flux for (2.8) may be written as

$$\hat{h}_{j+1/2}^{MLW} = \hat{f}_{j+1/2} + \frac{1}{2}\left[\varphi\left(r_{j+1/2}^{+LW}\right)\hat{g}_{j+1/2}^{+LW} - \varphi\left(r_{j+1/2}^{-LW}\right)\hat{g}_{j+1/2}^{-LW}\right], \tag{2.10}$$

where

$$\begin{aligned} \hat{g}_{j+1/2}^{+LW} &= (1 - \lambda a_{j+1/2}^{+})(f_{j+1}^{+} - f_j^{+}), \\ \hat{g}_{j+1/2}^{-LW} &= (1 + \lambda a_{j+1/2}^{-})(f_{j+1}^{-} - f_j^{-}), \end{aligned} \tag{2.11}$$

and the slope ratios should be redefined by

$$r_{j+1/2}^{+LW} = \hat{g}_{j-1/2}^{+LW}/\hat{g}_{j+1/2}^{+LW}, \quad r_{j+1/2}^{-LW} = \hat{g}_{j+3/2}^{-LW}/\hat{g}_{j+1/2}^{-LW}. \tag{2.12}$$

Here an appropriate flux splitting is needed that satisfies

$$\begin{aligned} f(u) &= f^{+}(u) + f^{-}(u), \\ a^{+} = \frac{df^{+}(u)}{du} \ge 0, &\quad a^{-} = \frac{df^{-}(u)}{du} \le 0, \end{aligned} \tag{2.13}$$

and the flux of the first-order upwind scheme takes the form

$$\hat{f}_{j+1/2} = f_j^{+} + f_{j+1}^{-}. \tag{2.14}$$

Clearly for a system of conservation laws, the set of eigenvalues of the Jacobian matrix is required, and field-by-field decompositions are necessary in order to apply the TVD algorithms scalarly to each of the characteristic equations.

2.2. *Modified Mac Cormack Scheme*

We have known the two-step schemes of Mac Cormack and Warming-Beam, which were originally devised for nonlinear cases and share the merits of not requiring Jacobian matrices for systems of conservation laws. Now we turn to conceive a new component-wise TVD technique by using these two well-known schemes.

The Mac Cormack scheme has two forms: one takes a forward difference in the predictor and a backward difference in the corrector; the other takes a backward difference in the predictor and a forward difference in the corrector. This enables us always to choose the first-order upwind scheme for the common predictor of the schemes of Mac Cormack and Warming-Beam.

Consider again the nonlinear scalar Eq. (2.7), for right-moving waves, i.e., $f^- \equiv 0$ in (2.13), we use the left upwind predictor for the above two schemes

$$\tilde{u}_j^{n+1} = u_j^n - \lambda \nabla f_j^n, \tag{2.15}$$

then their correctors have the following forms, respectively,

MC$^+$

$$u_j^{n+1} = \frac{1}{2}\left(u_j^n + \tilde{u}_j^{n+1}\right) - \frac{\lambda}{2}\Delta \tilde{f}_j^{n+1}, \tag{2.16a}$$

WB$^+$

$$u_j^{n+1} = \frac{1}{2}\left(u_j^n + \tilde{u}_j^{n+1}\right) - \frac{\lambda}{2}\nabla^2 f_j^n - \frac{\lambda}{2}\nabla \tilde{f}_j^{n+1}, \tag{2.16b}$$

where $\Delta(\cdot)_j = (\cdot)_{j+1} - (\cdot)_j$, $\nabla(\cdot)_j = (\cdot)_j - (\cdot)_{j-1}$. For linear case (2.1), $f_j^n = a u_j^n$, $\tilde{f}_j^{n+1} = a\tilde{u}_j^{n+1}$, it is easily verified that the Mac Cormack scheme (2.15) with (2.16a) is identical to the Lax–Wendroff scheme (2.2).

Likewise, for left-moving waves, i.e., $f^+ \equiv 0$ in (2.13), we use the right upwind predictor for both the schemes of Mac Cormack and Warming-Beam

$$\tilde{u}_j^{n+1} = u_j^n - \lambda \Delta f_j^n, \tag{2.17}$$

then their correctors have the following forms, respectively,

MC$^-$

$$u_j^{n+1} = \frac{1}{2}\left(u_j^n + \tilde{u}_j^{n+1}\right) - \frac{\lambda}{2}\nabla \tilde{f}_j^{n+1}, \tag{2.18a}$$

WB$^-$

$$u_j^{n+1} = \frac{1}{2}\left(u_j^n + \tilde{u}_j^{n+1}\right) + \frac{\lambda}{2}\Delta^2 f_j^n - \frac{\lambda}{2}\Delta \tilde{f}_j^{n+1}. \tag{2.18b}$$

When both left-moving and right-moving waves are coexisting, a flux splitting of (2.13) is also needed. Substitute the predictors of (2.15) and (2.17) for $\tilde{u}_j^{n+1}$ in their relevant correctors, and rewrite the upward schemes in the conservative form of (2.8); then we get an

extremely simple form of the numerical fluxes of the schemes for a general nonlinear scalar conservation law

$$\hat{h}^{MC}_{j+1/2} = \hat{f}_{j+1/2} + \frac{1}{2}\left[\hat{g}^{+MC}_{j+1/2} - \hat{g}^{-MC}_{j+1/2}\right], \tag{2.19a}$$

$$\hat{h}^{WB}_{j+1/2} = \hat{f}_{j+1/2} + \frac{1}{2}\left[\hat{g}^{+WB}_{j+1/2} - \hat{g}^{-WB}_{j+1/2}\right], \tag{2.19b}$$

where

$$\hat{g}^{+MC}_{j+1/2} = \tilde{f}^{+}_{j+1} - f^{+}_{j}, \quad \hat{g}^{-MC}_{j+1/2} = f^{-}_{j+1} - \tilde{f}^{-}_{j}, \tag{2.20a}$$

$$\hat{g}^{+WB}_{j+1/2} = \tilde{f}^{+}_{j} - f^{+}_{j-1}, \quad \hat{g}^{-WB}_{j+1/2} = f^{-}_{j+2} - \tilde{f}^{-}_{j+1}. \tag{2.20b}$$

It is obvious that $\hat{g}^{+WB}_{j+1/2} = \hat{g}^{+MC}_{j-1/2}$, $\hat{g}^{-WB}_{j+1/2} = \hat{g}^{-MC}_{j-1/2}$, and $\hat{h}^{WB}_{j+1/2} = \hat{h}^{MC}_{j-1/2}$. Following the flux limiting procedure of the modified Lax–Wendroff scheme in Sec. 2.1, by adding a pure flux limiter to the second-order antidiffusive term of (2.19), we get a modified second-order predictor-corrector scheme, namely the modified Mac Cormack scheme

$$\tilde{u}^{n+1}_{j} = u^{n}_{j} - \lambda\left(\hat{f}_{j+1/2} - \hat{f}_{j-1/2}\right), \tag{2.21a}$$

$$u^{n+1}_{j} = u^{n}_{j} - \lambda\left(\hat{h}^{MMC}_{j+1/2} - \hat{h}^{MMC}_{j-1/2}\right), \tag{2.21b}$$

$$\hat{h}^{MMC}_{j+1/2} = \hat{f}_{j+1/2} + \frac{1}{2}\left[\varphi\left(r^{+MC}_{j+1/2}\right)\hat{g}^{+MC}_{j+1/2} - \varphi\left(r^{-MC}_{j+1/2}\right)\hat{g}^{-MC}_{j+1/2}\right], \tag{2.21c}$$

where $\hat{f}_{j+1/2}$ is defined by (2.14), and the slope ratio is redefined by

$$r^{+MC}_{j+1/2} = \hat{g}^{+MC}_{j-1/2}/\hat{g}^{+MC}_{j+1/2}, \quad r^{-MC}_{j+1/2} = \hat{g}^{-MC}_{j+3/2}/\hat{g}^{-MC}_{j+1/2}. \tag{2.22}$$

Obviously $\varphi(r) = 1$ or $\varphi(r) = r$ switches the formulae of (2.21) to the Mac Cormack scheme and the Warming-Beam scheme, respectively.

2.3. *Component-Wise TVD Procedure*

For the modified Mac Cormack scheme of (2.21), all the negative flux terms vanish in the linear case of (2.1), and then the scheme degenerates to the formula of (2.3) which is absolutely TVD under the condition of (2.5). However, for the nonlinear case, we may as well refer to the resulting scheme as a two-step TVD scheme whenever a pure flux limiter $\varphi(r)$ bounded by the usual TVD constraint of (2.6) is applied to the modified Mac Cormack scheme; although it is impossible to be abstractly proved up to now.

The two-step TVD scheme does not need to use the set of eigenvalues of the Jacobian matrix, but an appropriate flux splitting is still required for its upwinding procedure. In this paper we choose the simplest and inexpensive global Lax–Friedrichs flux splitting [13]

$$f^{\pm}_{j}(u) = \frac{1}{2}\left(f(u_j) \pm \alpha u_j\right), \tag{2.23a}$$

where α, also required by the *CFL* number, is taken as the maximum eigenvalue of $f(u)$ over the relevant range of u

$$\alpha = \max_j |f'(u_j)|. \tag{2.23b}$$

Of course, a less dissipative local Lax–Friedrichs splitting is also available

$$f_j^{\pm}(u) = \frac{1}{2}(f(u_j) \pm \alpha_j u_j), \tag{2.24a}$$

where

$$\alpha_j = |f'(u_j)|. \tag{2.24b}$$

But in our experiences, we found it not robust enough compared with the global algorithm.

The one-dimensional Euler system may be written as

$$U_t + F(U)_x = 0, \tag{2.25}$$

where

$$U = (\rho, \rho u, E)^T, \tag{2.26a}$$

$$F(U) = (\rho u, \rho u^2 + P, u(E + P))^T. \tag{2.26b}$$

Here ρ is the density, u is the velocity, E is the total energy, and P is the pressure. Then the parameter α in the global Lax–Friedrichs flux splitting can be taken as the maximum speed of entropy waves

$$\alpha = \max_j(|u_j| + c_j), \tag{2.27}$$

where c_j is the local sound speed. For the Euler system, there are many other flux splittings (e.g., van Leer [18]). In view of monotonicity, robustness, and applicability to complicated equation of state, we prefer the global Lax–Friedrichs flux (2.23a) and (2.27). Under these circumstances, we then approximate the Euler system via a component-by-component TVD limiting without any difficulties.

Many TVD limiters were well investigated in the literatures [2–7]. Usually a compressive limiter (e.g., superbee [3]) gives excellent resolution of discontinuities but simultaneously turns smooth data into staircase. Comparatively a harmonic limiter is more reliable especially for the nonlinear case. We noted three of such limiters—Roe's symmetric limiter φ_H [4], Hartwich's antisymmetric limiter φ_A [5], and the minmod limiter φ_M

$$\varphi_H(r) = \begin{cases} r, & |r| < 1, \\ 1, & \text{otherwise}, \end{cases} \tag{2.28a}$$

$$\varphi_A(r) = \text{sign}(r) \cdot \min(|r|,\ 1), \tag{2.28b}$$

$$\varphi_M(r) = \text{Minmod}(r,\ 1). \tag{2.28c}$$

The three limiters differ only when the slope ratio r turns negative, but we can hardly see their differences in numerical tests even near extrema (i.e., $r < 0$). Practically the limiter φ_H is identical to the minimum of the absolute value function used in ENO schemes

$$M(a,b) = \begin{cases} a, & |a| < |b|; \\ b, & \text{otherwise.} \end{cases} \tag{2.29}$$

For the sake of symmetry and comparing with ENO schemes, we choose the limiter φ_H for all the calculations of the present paper.

3. NUMERICAL RESULTS

Since the scheme degenerates to a usual TVD scheme in the linear case, we apply it directly to nonlinear conservation laws.

3.1. *Single Conservation Law*

EXAMPLE 1. Initial value problem for Burgers equation

$$\begin{aligned} u_t + \left(\frac{u^2}{2}\right)_x &= 0, \\ u(x,0) &= \begin{cases} -1, & x < -0.5; \\ 1, & -0.5 \le x \le 0.5; \\ -1, & x > 0.5. \end{cases} \end{aligned} \tag{3.1}$$

Its solution consists of a centered rarefaction wave that contains a sonic point at $x = -0.5$ and a stationary shock wave located at $x = 0.5$. Many conventional TVD schemes (if without any entropy fix added) would substitute the rarefaction wave by an nonphysical stationary expansion shock [16]. Figure 1 shows the numerical solutions obtained by using our component-wise TVD scheme. We can see that the centered rarefaction wave converges to the correct entropy solution and the stationary shock is well resolved.

3.2. *Euler System in One Dimension*

Next we consider the one-dimensional Euler equations for a polytropic ideal gas (perfect gas) with the equation of state

$$P = (\gamma - 1)\rho\varepsilon, \tag{3.2}$$

where $\varepsilon = \frac{E}{\rho} - \frac{1}{2}u^2$ is the internal energy per unit mass and $\gamma = 1.4$. We then applied the component-wise TVD algorithm scalarly to each of the three conservation equations.

EXAMPLE 2. Low density problem [8] with the initial data

$$\begin{aligned} (\rho_L, u_L, P_L) &= (1, -2, 0.4), \quad x \le 0; \\ (\rho_R, u_R, P_R) &= (1, 2, 0.4), \quad x > 0. \end{aligned}$$

The solution of this problem consists of two strong rarefaction waves moving in opposite directions. The numerical results at $t = 0.1$ are depicted in Fig. 2. Since the energy of

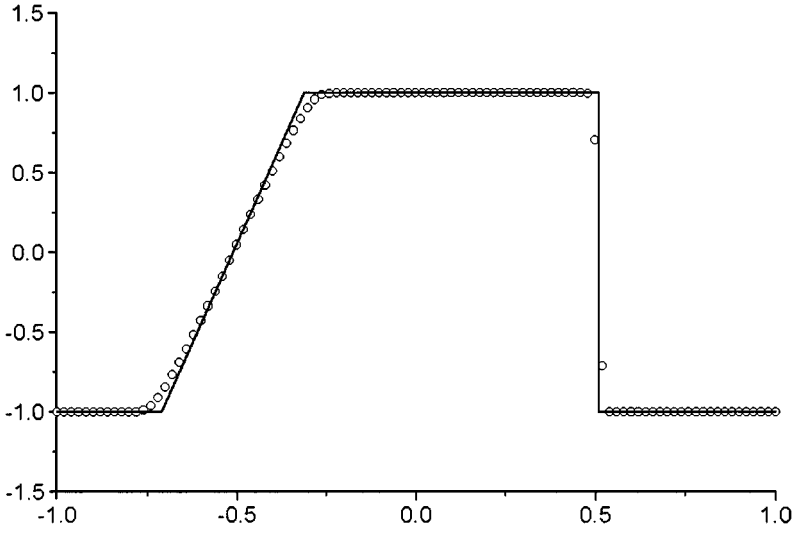

FIG. 1. Approximations of the component-wise TVD scheme to a solution of Burgers equation containing a transonic shock and a transonic rarefaction. $dx = 1/50$, $CFL = 0.8$, $t = 0.2$.

the flow is largely kinetic, many conservative differencing schemes may fail by predicting nonphysical states with negative density or internal energy (see [8]). In Fig. 2 we can see that our scheme solves this problem without any difficulties.

EXAMPLE 3. Sod's shock tube problem with the initial data

$$(\rho_L, u_L, P_L) = (1, 0, 1), \qquad x \le 0;$$
$$(\rho_R, u_R, P_R) = (0.125, 0, 0.1), \quad x > 0.$$

Figure 3 shows the numerical results compared with the exact solution (solid lines) at $t = 2.5$. We use 100 grid points on the domain $[-5, 5]$ with $CFL = 0.8$. In the figure, the results of the second-order, component-wise, efficient ENO schemes [13] are also shown (solid diamonds); the open circles are of the present scheme. It is found that shocks are captured sharply by the present scheme without any oscillations though the contact discontinuity is somewhat dissipative.

EXAMPLE 4. Shu–Osher's problem of shock entropy wave interactions [11] with the following initial conditions:

$$\rho = 3.85714, \quad u = 2.629369, \quad P = 10.33333, \quad x \le -4;$$
$$\rho = 1 + 0.2\sin(5x), \quad u = 0, \quad P = 1, \quad x > -4.$$

The mean flow of the problem is a pure right moving Mach 3 shock. With a small disturbance of sine waves coupled in density, the flow field brings about both shocks and complicated smooth features coexisting. We require 200 grid points per wavelength with $CFL = 0.8$. Figure 4 shows the numerical results of density compared with the exact solution (solid lines) at $t = 1.8$. Figure 4 (top) is again the results of the second-order,

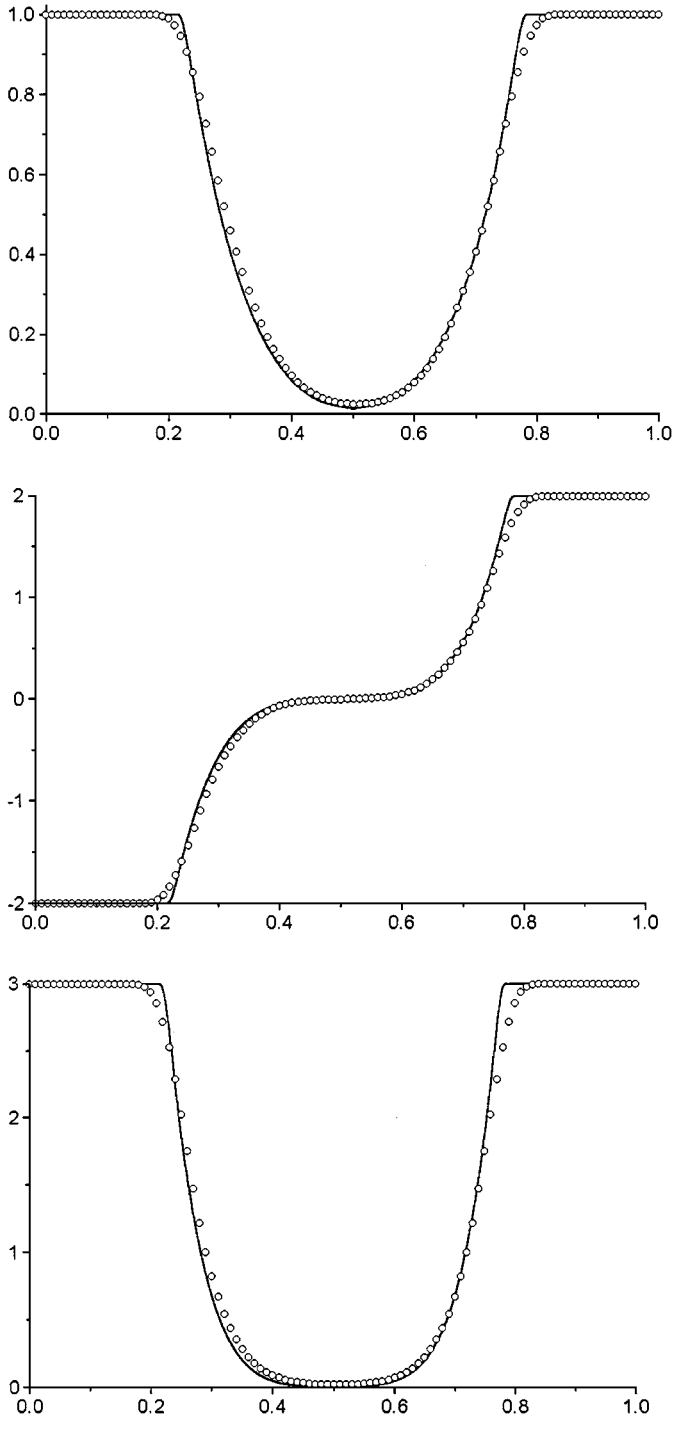

FIG. 2. Low density problem with component-wise TVD, 100 points, $CFL = 0.8$, $t = 0.1$, (top) density, (middle) momentum, (bottom) internal energy.

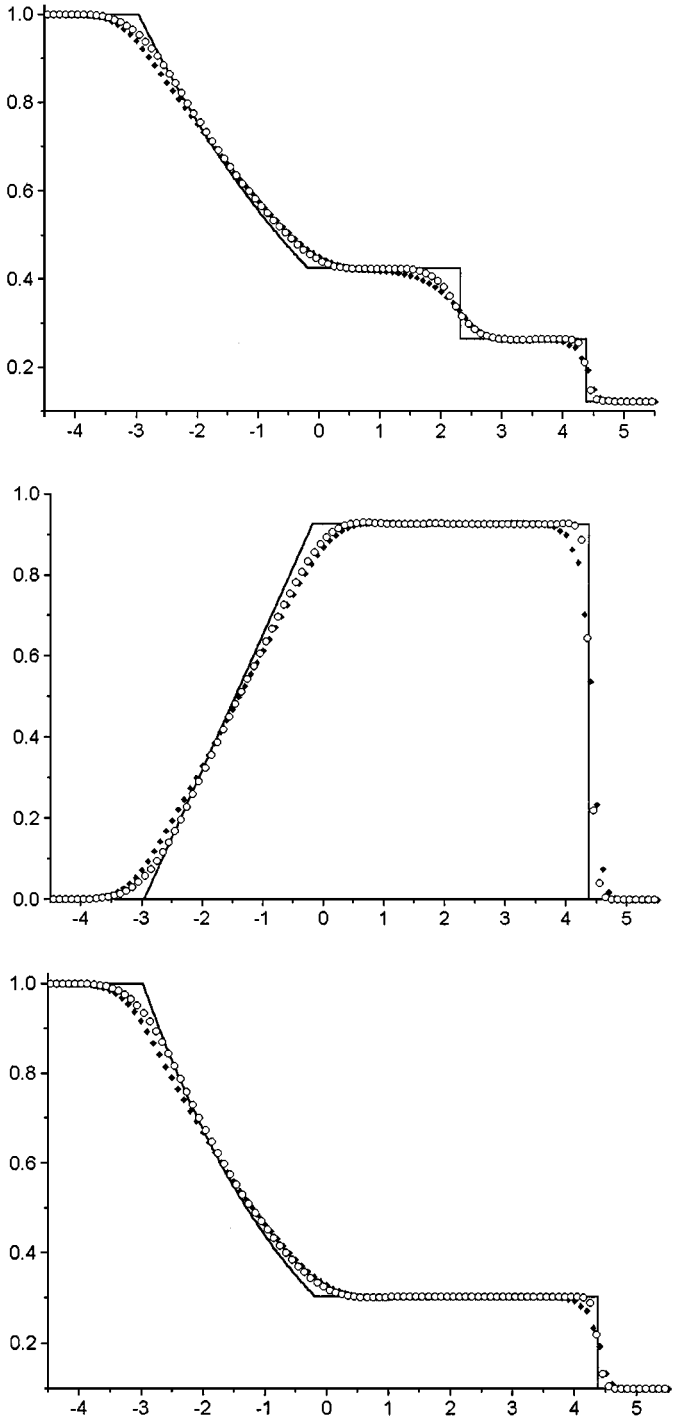

FIG. 3. Sod shock tube problem with component-wise TVD (the solid diamonds are of the second-order component-wise ENO scheme), 100 points, $CFL = 0.8, t = 2.5$, (top) density, (middle) velocity, (bottom) pressure.

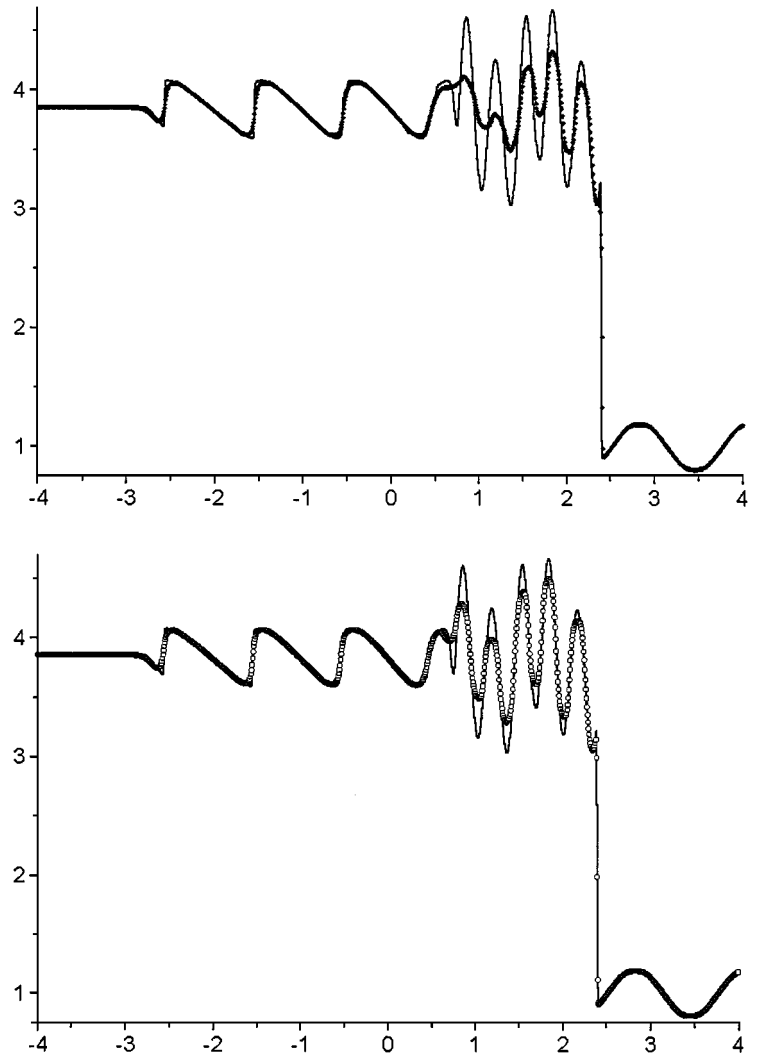

FIG. 4. Shock entropy wave interactions problem, 200 points per wavelength, $CFL = 0.8$, $t = 1.8$, solid lines are exact solution of density, (top) second-order component-wise ENO, (bottom) component-wise TVD.

component-wise ENO schemes, and Fig. 4 (bottom) is of the present scheme. It is gratifying to see that both shocks and fine structures of smooth regions are resolved very well.

From Figs. 3 and 4, we find that the present, component-wise TVD scheme is less dissipative than the ENO schemes under the same circumstances. This reflects the superiority of the Mac Cormack-type schemes.

EXAMPLE 5. Lax's shock tube problem: Initial data are

$$(\rho_L, u_L, P_L) = (0.445, 0.698, 3.528), \quad x \le 0;$$
$$(\rho_R, u_R, P_R) = (0.5, 0, 0.571), \quad x > 0.$$

Figure 5 shows the numerical results compared with the exact solution (solid lines) at $t = 1.5$. We used 200 grid points on the domain $[-5, 5]$ with $CFL = 0.8$. This time we compared our component-wise technique with the field-by-field decomposition limiting. In

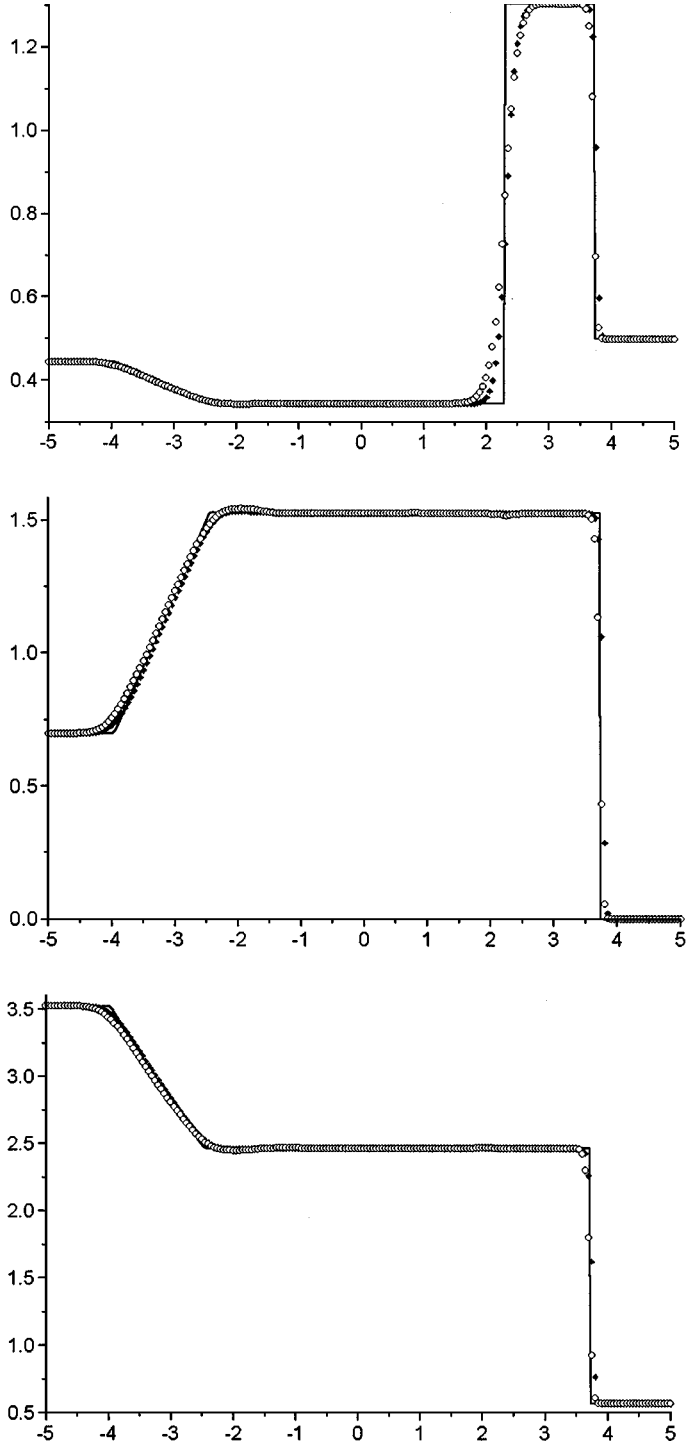

FIG. 5. Lax shock tube problem with component-wise TVD (the solid diamonds are of the second-order characteristic-based TVD scheme), 200 points, $CFL = 0.8$, $t = 1.5$, (top) density, (middle) velocity, (bottom) pressure.

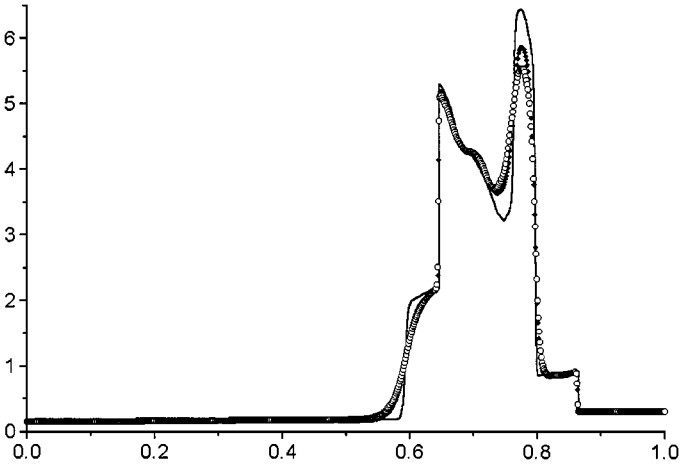

FIG. 6. Two interacting blast wave problem, 800 points, $CFL = 0.8, t = 0.038$, solid lines are the exact solution, the solid diamonds are of van Leer flux splitting, and the open circles are of the local Lax–Friedrichs flux splitting.

the figure, we show the results of the conventional second-order TVD scheme based on the Roe solver (also with the Roe's symmetric limiter φ_H). The present component-wise TVD scheme is a bit more dissipative than the characteristic-based TVD scheme. But the latter costs fully twice the computing time of our method.

EXAMPLE 6. Two interacting blast waves: The initial data are

$$(\rho, u, P) = \begin{cases} (1, 0, 1000), & 0 \le x \le 0.1; \\ (1, 0, 0.01), & 0.1 < x < 0.9; \\ (1, 0, 100), & 0.9 \le x \le 1. \end{cases}$$

Reflecting boundary conditions are applied at both ends. In Fig. 6 we show the numerical results of the component-wise TVD scheme using the local Lax–Friedrichs flux (2.24) and van Leer flux [18], respectively. It is found that the van Leer flux is less dissipative than the local Lax–Friedrichs flux in this example. Showing this example may inspire the reader to explore better forms of flux splitting.

3.3. *Euler System in Two Dimensions*

The next two examples are of two-dimensional Euler systems. We extend the component-wise TVD scheme by the method of fractional steps or time splitting.

EXAMPLE 7. Forward facing step problem: It has been carefully examined in [9] and is acknowledged as a standard test case for high-resolution schemes in two-dimensional space. The wind tunnel is 1 length unit wide and 3 length units long. The step is 0.2 length units high and is located 0.6 length units from the left-hand end of the tunnel. A right-moving Mach 3 flow is continuously fed from the entrance (left-hand end). An assumption of a nearly steady flow in the region near the corner is applied (see [9] and [16] for details). In Fig. 7 we present the numerical results of the new TVD scheme with 240×80 grid points. We can see that both strong shocks and strong centered rarefaction waves are resolved very well.

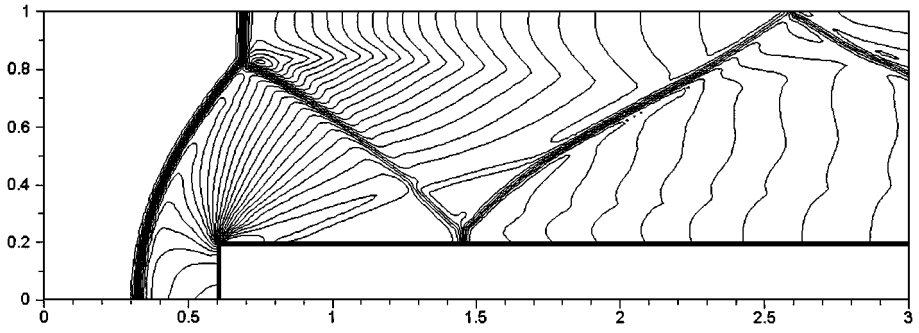

FIG. 7. Flow past a forword facing step with component-wise TVD, 30 contours of density from 0.434 to 6.417. $\Delta x = \Delta y = 1/80$, $CFL = 0.8$, $t = 4$.

EXAMPLE 8. Double Mach reflection problem: This is again a standard test case for high-resolution schemes. A Mach 10 planar air shock is incident on an oblique wedge at a 60° angle. The reflecting wall of the wedge lies at the bottom of the computational domain starting from $x = 1/6$. A detailed description of this problem can be found in [9]. Figure 8 (top) shows quite pleasing results of the present component-wise TVD scheme with 480×120 grid points in the domain: $[0, 4] \times [0, 1]$.

EXAMPLE 9. Double Mach reflection in real gas: Here all conditions are the same as those in Example 8 except that the polytropic ideal gas is changed to the two-molecular vibrating gas (see [15]). The equation of state becomes

$$P = r\rho T(\varepsilon), \tag{3.3}$$

where ε is the specific internal energy and the temperature T is given by the implicit expression

$$\varepsilon = C_v^{tr} T + \frac{\alpha \Theta_{\text{vib}}}{\exp(\Theta_{\text{vib}}/T) - 1}, \tag{3.4}$$

with $r = 287.086 J \cdot kg^{-1} \cdot K^{-1}$, $C_v^{tr} = r/(\gamma_{tr} - 1)$, $\gamma_{tr} = 1.4$, $\Theta_{\text{vib}} = 10^3 K$, and $\alpha = r$.

A strict field-by-field decomposition is impossible for this complicated coupled Euler system. But our component-wise TVD algorithm has no difficulty solving this problem. Figure 8 (middle & bottom) shows the numerical results of this real gas model compared with that of the perfect gas model. 960×240 grid points are used in the domain: $[0, 4] \times [0, 1]$. We can see that the main shock is closer to the bottom boundary and the shock below the triple point bends.

4. DISCUSSION AND CONCLUSIONS

Through the combination of the Mac Cormack scheme and the Warming-Beam scheme, we propose a two-step, component-wise TVD scheme for nonlinear conservation laws. The performances of the new scheme are quite pleasing on a lot of numerical experiments.

The two-step scheme employs component-wise limiting and takes the predictor of the first-order upwinding; hence it is more economical in computation. For the approximations

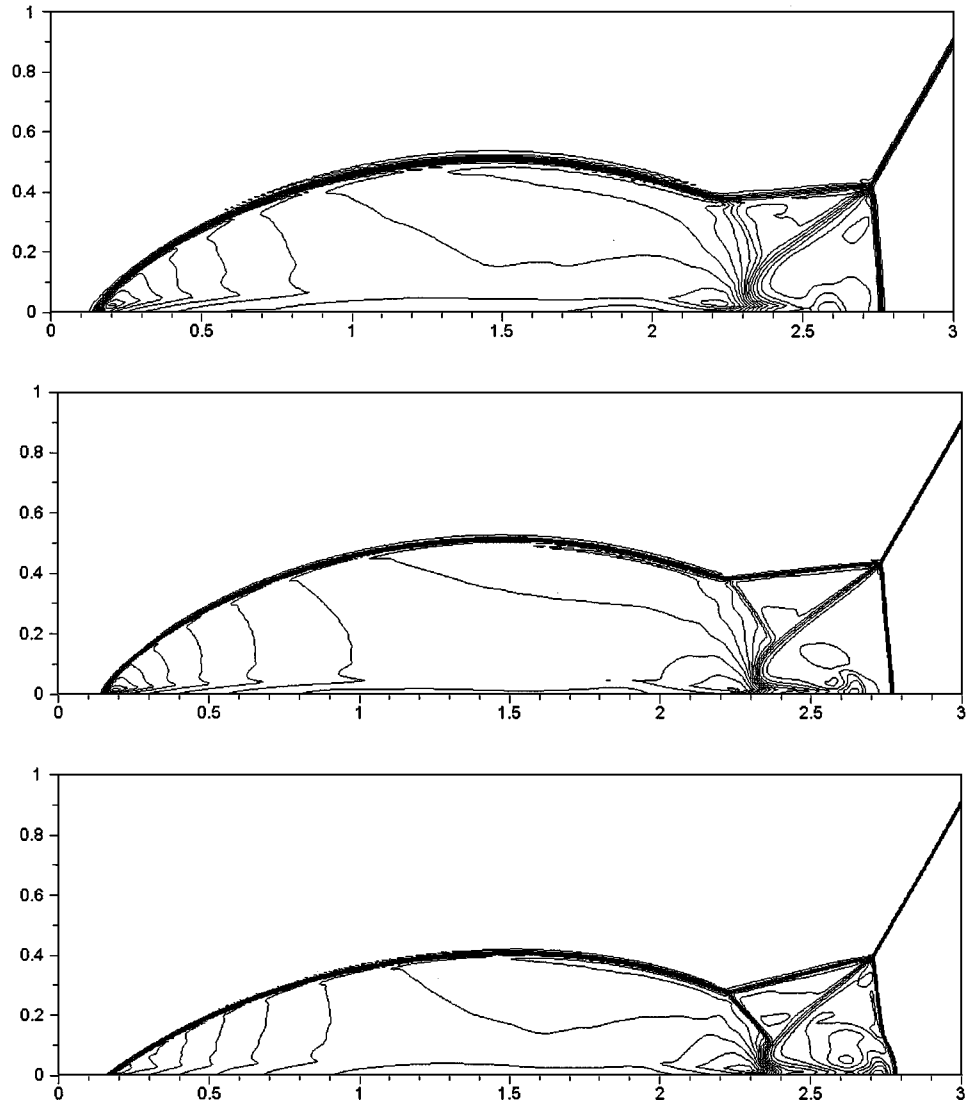

FIG. 8. Double Mach reflection with component-wise TVD, 30 contours of density, $CFL = 0.8$, $t = 0.2$. (top) perfect gas, $\Delta x = \Delta y = 1/120$, density from 1.4 to 20.64; (middle) perfect gas, $\Delta x = \Delta y = 1/240$, density from 1.4 to 21.63; (bottom) real gas, $\Delta x = \Delta y = 1/240$, density from 1.4 to 31.22.

to Euler systems, we found the scheme is two times faster than the usual TVD schemes based on field-by-field decomposition limiting; moreover, we found the scheme runs even a bit faster than the second-order, component-wise ENO schemes. We expect that higher-order multi-step TVD schemes of this kind would fully unfold their advantages of lower computational costs.

The scheme does not necessiate the characteristic decompositions; hence its programming is very simple. The approximations to a real gas system show only a fraction of its abilities to handle with complicated coupled systems.

Although the scheme is second-order accurate (first-order near extrema), it exhibits even higher accuracy over the same order component-wise ENO schemes. This reflects the

superiority of the Mac Cormack-type schemes. Of course, the two-step, component-wise TVD scheme will perform better if a better component-wise flux is devised which is closer to that of the field-by-field decomposition.

ACKNOWLEDGMENTS

The authors thank professor Hongshou Shui for helpful discussions. This work was supported by the specific fund of higher educational doctoral program (98024627) and the pre-research fund of Chinese Academy of Engineering Physics (20010659).

REFERENCES

1. A. Harten, High resolution schemes for hyperbolic conservation laws, *J. Comput. Phys.* **49**, 357 (1983).
2. P. K. Sweby, High resolution schemes using flux limiters for hyperbolic conservation laws, *SIAM J. Numer. Anal.* **21**, 995 (1984).
3. P. L. Roe, Some contributions to the modeling of discontinuous flows, in *Lectures in Applied Mathematics*, (1985), Vol. 22, p. 163.
4. P. L. Roe, A Survey of Upwind Differencing Techniques, Lecture Notes in Physics **323**, 69–78 (1989).
5. P.-M. Hartwich, C.-H. Hsu, and C. H. Liu, *Total Variation Diminishing (TVD) Schemes of Uniform Accuracy*, NASA-TM-100552 (1988).
6. Y. N. Jeng and U. J. Payne, An adaptive TVD limiter, *J. Comput. Phys.* **118**, 229 (1995).
7. Mohit Arora and Philip L. Roe, A well-behaved TVD limiter for high resolution calculations of unsteady flow, *J. Comput. Phys.* **132**, 3 (1997).
8. B. Einfeldt, C. D. Munz, P. L. Roe, and B. Sjogreen, On Godunov-type methods near low densities, *J. Comput. Phys.* **92**, 273 (1991).
9. P. Woodward and P. Colella, The numerical simulation of two-dimensional fluid flow with strong shocks, *J. Comput. Phys.* **54**, 115 (1984).
10. R. Hannappel, T. Hauser, and R. Friedrich, A comparison of ENO and TVD schemes for the computation of shock-turbulence interaction, *J. Comput. Phys.* **121**, 176 (1995).
11. A. Harten, B. Engquist, S. Osher, and R. Chakravarthy, Uniformly high-order accurate essentially non-oscillatory schemes III, *J. Comput. Phys.* **71**, 231 (1987).
12. C. W. Shu and S. Osher, Efficient implementation of essentially non-oscillatory shock-capturing schemes II, *J. Comput. Phys.* **83**, 32 (1989).
13. C. W. Shu, *Essentially Non-Oscillatory and Weighted Essentially Non-Oscillatory Schemes for Hyperbolic Conservation Laws*, ICASE Report No. 97-65 (1997).
14. X. D. Liu and S. Osher, Convex ENO high order multi-dimensional schemes without field by field decomposition or staggered grids, *J. Comput. Phys.* **142**, 304 (1998).
15. P. Montarnal and C. W. Shu, Real gas computation using an energy relaxation method and high-order WENO schemes, *J. Comput. Phys.* **148**, 59 (1999).
16. R. Donat and A. Marquina, Capturing shock reflections: An improved flux formula, *J. Comput. Phys.* **125**, 42 (1996).
17. J. J. Quirk, A contribution to the great Riemann solver debate, *Int. J. Numer. Meth. Fluids* **18**, 555 (1994).
18. B. van Leer, Towards the ultimate conservative difference scheme: A second-order sequel to Godunov's method, *J. Comput. Phys.* **32**, 101 (1979).
19. H. C. Yee, Construction of explicit and implicit symmetric TVD schemes and their applications, *J. Comput. Phys.* **68**, 151 (1987).